Available online at www.sciencedirect.com
SCIENCE DIRECT®
Journal of Structural Biology 152 (2005) 28–35
Journal of Structural Biology
www.elsevier.com/locate/yjsbi

Localization of the PsbH subunit in photosystem II from the *Synechocystis* 6803 using the His-tagged Ni–NTA Nanogold labeling

Ladislav Bumba [a,b,*], Martin Tichy [c,d], Marika Dobakova [c,d], Josef Komenda [c,d], Frantisek Vacha [a,c]

[a] *Institute of Plant and Molecular Biology, Czech Academy of Sciences, Branisovska 31, 370 05 Ceské Budejovice, Czech Republic*
[b] *Laboratory of Molecular Biology of Bacterial Pathogens, Institute of Microbiology, Videnska 1083, 142 20 Prague, Czech Republic*
[c] *Institute of Physical Biology, University of South Bohemia, Zamek 136, 373 33 Nove Hrady, Czech Republic*
[d] *Laboratory of Photosynthesis, Institute of Microbiology, Academy of Sciences, 379 81 Trebon, Czech Republic*

Received 25 May 2005; received in revised form 27 July 2005; accepted 3 August 2005
Available online 31 August 2005

Abstract

The PsbH protein belongs to a group of small protein subunits of photosystem II (PSII) complex. This protein is predicted to have a single transmembrane helix and it is important for the assembly of the PSII complex as well as for the proper function at the acceptor side of PSII. To identify the location of the PsbH subunit, the PSII complex with His-tagged PsbH protein was isolated from the cyanobacterium *Synechocystis* sp. PCC 6803 and labeled by Ni^{2+}–nitrilo triacetic acid Nanogold. Electron microscopy followed by single particle image analysis identified the location of the labeled His-tagged PsbH protein at the periphery of the dimeric PSII complex. These results indicate that the N terminus of the PsbH protein is located at the stromal surface of the PSII complex and close to the CP47 protein.

Keywords: Electron microscopy; Photosystem II; PsbH protein; Immunogold labeling

1. Introduction

Oxygenic photosynthesis is a process in which plants, algae and cyanobacteria use light energy to drive the synthesis of organic compounds and produce all molecular oxygen, necessary for aerobic life on Earth. The light-harvesting and energy-transducing functions of oxygenic photosynthesis are localized in specialized photosynthetic membranes, thylakoids, and carried out by several types of protein complexes embedded in the membrane. Central to this process is photosystem II (PSII) complex that catalyzes the light-induced production of oxygen, thereby transferring electrons from water to plastoquinone. The PSII complex is dimer and contains more than 25 subunits per monomer (Hankamer et al., 2001a). All redox cofactors are bound to the central part of the complex formed by the reaction center D1 and D2 proteins. The reaction center is surrounded by the so-called inner antenna proteins CP43 and CP47, and several low molecular mass subunits each predicted to have a single transmembrane helix.

PsbH protein belongs to a group of small protein subunits of the PSII complex. The PsbH protein was originally detected as a 10 kDa phosphoprotein (Bennet, 1977) and subsequently sequenced in number of prokaryotic and eukaryotic organisms (recently reviewed by Komenda et al., 2003). The PsbH protein is predicted to have single transmembrane helix with its 72 amino acid residues in higher plants (Shinozaki et al., 1986) and 87 amino acid residues in the green alga *Chlamydomonas reinhardtii* (Dedner et al., 1988).

* Corresponding author. Fax: +42 03 85 31 03 56.
E-mail address: bumba@seznam.cz (L. Bumba).

1047-8477/$ - see front matter © 2005 Elsevier Inc. All rights reserved.
doi:10.1016/j.jsb.2005.08.001

In higher plants and green algae the PsbH protein undergoes reversible phosphorylation at two threonine residues close to the N terminus (Michel and Bennett, 1987; Vener et al., 2001). The cyanobacterial PsbH protein is truncated at its N terminus and misses these phosphorylation sites (Mayes and Barber, 1991). The function of PsbH protein in PSII complex has been associated, through analysis of a *Synechocystis* mutant lacking the coding gene, with control of the electron flow from Q_A to Q_B (Mayes et al., 1993), protection from photoinhibition (Komenda and Barber, 1995), and bicarbonate binding on its acceptor site (Komenda et al., 2002). However, disruption of the PsbH subunit in *C. reinhardtii* led to the disappearance of PSII from thylakoid membrane (O'Connor et al., 1998; Summer et al., 1997).

Recently, three-dimensional (3-D) structures of the PSII core complex have been solved by X-ray (Ferreira et al., 2004; Kamiya and Shen, 2003; Zouni et al., 2001) and electron crystallography (Hankamer et al., 2001b). The models show that the overall organization of 22 transmembrane helices of the major PSII subunits (CP47, CP43, D1, and D2) is preserved between higher plant and cyanobacteria. In addition, 12 (spinach) and 14 (cyanobacteria) low molecular mass subunits, each predicted to have single membrane-spanning α-helix, were identified in each monomer of the dimeric PSII complex. Of them only PsbE and PsbF, as components of cytochrome (cyt) b_{559}, were identified by locating the haem group near to D2 protein of the D1/D2 reaction center complex. So far, the assignment of the smaller subunits in PSII is not certain and have been based on chemical cross-linking studies (Büchel et al., 2001; Hankamer et al., 2001a), immunogold labeling experiments (Bumba and Vácha, 2003) or comparative studies of wild type with mutants depleted of the smaller PSII proteins (Komenda et al., 2002; Shi et al., 2000; Swiatek et al., 2001). Unfortunately, to date, all attempts to work out the location of the small subunits rationally have generated contradictory information (Shi and Schröder, 2004). Recently, Büchel et al. (2001) identified the location of the PsbH subunit in PSII core complex from *C. reinhardtii* using a His-tagged PsbH mutant and gold labeling. Here, we describe the Ni^{2+}–nitrilo triacetic acid (Ni–NTA) Nanogold labeling of the PsbH subunit in the PSII core complex isolated from the His-tagged PsbH mutant of the cyanobacterium *Synechocystis* 6803. The gold label consists of a gold cluster coupled to Ni–NTA Nanogold that has a high binding affinity to multiple histidine residues of the His-tagged protein (Hainfeld et al., 1999). In combination of single particle analysis of Ni–NTA Nanogold labeled PSII particles and molecular modeling of known X-ray coordinates of the PSII structure we were able to suggest the location of the PsbH subunit within the PSII complex.

2. Materials and methods

2.1. Mutant construction

The *Synechocystis* 6803 PsbH-His strain with PsbH protein tagged with the His_6 epitope on its N terminus expressed under psbA2 promoter has been constructed. *PsbH* gene was amplified by PCR using the mix of *Taq* and *Pfu* DNA polymerases and gene specific primers with artificially generated restriction sites for *Nde*I and *Bam*HI and containing six histidine codons (CAT) in the forward primer. After restriction, the PCR fragment was cloned into *Nde*I and *Bam*HI sites of the pSBA plasmid containing the upstream and downstream regions of the *Synechocystis* 6803 *psb*AII gene (Lagarde et al., 2000). Ligation mix was amplified by PCR using the pSBA primers amplifying the whole *psbA*/*psbH-His* region. Amplification by PCR was chosen because transformation of *Escherichia coli* with the ligation mix repeatedly yielded no colonies. The PCR product containing *psb*H-His gene was transformed into *Synechocystis* 6803 psbAII-KS strain where the psbA2 gene was replaced by kanamycin-resistance/*sacB* cartridge (Lagarde et al., 2000). The *sacB* gene is coding for levan sucrase leading to sucrose sensitivity of this strain. After transformation, *Synechocystis* cells were grown on BG-11 plates for four days. Transformants were than transferred to plates with 5% sucrose and sucrose resistant colonies were checked for kanamycin sensitivity. Resulting strain expressing both wild type and His tagged forms of PsbH protein has been transformed with chromosomal DNA from $PsbH^-$ strain (Mayes et al., 1993). Deletion of wild type copy of *psbH* gene in PsbH-His strain was confirmed by PCR.

2.2. Isolation of thylakoid membranes

Cells were harvested in the exponential growth phase, resuspended in thylakoid buffer (50 mM MES/NaOH, pH 6.5) and broken in a *MiniBeadBeater* (BioSpec Products, USA) by three breaking cycles (30 s shaking followed by a 3 min cooling on ice). After centrifugation at 2000*g* for 1 min to remove cell debris, the supernatant was centrifuged in at 30,000*g* for 10 min at 4 °C. Thylakoid membranes were resuspended in thylakoid buffer.

2.3. Isolation of PSII complex

Thylakoid membranes were solubilized with 1% dodecyl-maltoside (DM) in thylakoid buffer with 100 mM NaCl at chlorophyll concentration of 1 mg ml^{-1} for 15 min. The unsolubilized material was removed by centrifugation for 30 min at 60,000 *g* and the supernatant was used for affinity chromatography on Fractogel EMD Chelate (Merck) charged with Ni^{2+}. The column was sequentially washed with thylakoid buffer–NaCl

with 5 and 25 mM imidazole. PSII was eluted by 50 mM imidazole. The PSII was further purified by gel filtration chromatography on Superdex 200HR 10/30 column (Amersham Biosciences) connected to a HPLC pump (LCP 3001, Ecom, Czech Republic) and photodiode array detector Waters 996 (Waters, USA). The column was equilibrated with 20 mM MES/NaOH (pH 6.5), 10 mM NaCl and 0.03% DM at flow rate of 0.5 ml/min (Bumba et al., 2004).

2.4. Polyacrylamide gel electrophoresis and Western blotting

Protein composition was determined by SDS–PAGE using a 12–20% linear gradient of polyacrylamide gel carried out using Tris/glycine gel containing 7 M urea. Gels were stained with Coomassie brilliant blue stain. After electrophoresis, proteins were transferred to *PVDF* membrane (*Hybond-P*, *Amersham Biosciences*) using wet blotting system. Blotted membranes were subjected to immunoblot analysis using the PsbH antibody (1:6000 dilution) or *polyHistine* antibody (*Sigma H 1029*, 1:3000 dilution). Primary antibody was detected with peroxidase-conjugated secondary antibody. PsbH antibody has been prepared in rabbit using PsbH-GST fusion protein expressed in *E. coli* as an antigen (Halbhuber et al., 2003).

2.5. Pigment analysis

Room temperature absorption spectra were recorded with a UV300 spectrophotometer (Spectronic Unicam, UK). Fluorescent emission spectra were measured at liquid nitrogen temperature using a Fluorolog spectrofluorometer (Jobin Yvon, USA) with an excitation wavelength of 430 nm.

2.6. Oxygen evolution

Oxygen evolution was measured using a Clark-type oxygen electrode (Hansatech). Samples at a chlorophyll concentration of 10 μg(Chl) ml^{-1} were suspended in a medium containing 20 mM MES (pH 6.5), 0.3 M sucrose, 20 mM $CaCl_2$, 10 mM $NaHCO_3$, 10 mM NaCl, supplemented with electron acceptors, 2,5-dichloro-*p*-benzoquinone at a concentration of 500 μM and ferrycyanide at a concentration of 2.5 mM and illuminated with saturating white light.

2.7. Electron microscopy and image analysis

Freshly prepared PSII complexes were placed on glow-discharged carbon coated copper grids and excessive liquid was removed using filter paper. The grid was then placed upside-down on a droplet of a Ni^{2+}-nitrilotriacetic acid Nanogold (Ni–NTA Nanogold) solution (Nanoprobes, USA). After 15 min incubation at room temperature the grid was removed from the droplet, rinsed with water and negatively stained with 0.75% uranyl acetate. Electron microscopy was performed with Philips TEM 420 electron microscope using 80 kV at 60,000× magnification. Micrographs free from astigmatism and drift were scanned with a pixel size corresponding to 4.5 Å at the specimen level. Image analyses were carried out using SPIDER software (Frank et al., 1996). From 85 micrographs of the PSII cores, about 3500 top-view projections of unlabeled particles and 260 top-view projections of labeled particles were selected for analysis. Both separate data sets were rotationally and translationally aligned, and treated with multivariate statistical analysis in combination with classification (Harauz et al., 1988; van Heel and Frank, 1981). Classes from each of the subsets were used for refinement of alignments and subsequent classifications. For the final sum, the best of the class member were summed, using a cross-correlation coefficient of the alignment procedure as a quality parameter. The resolution of the images was calculated by using the Fourier ring correlation method (van Heel, 1987). For molecular modeling, the coordinates were taken from Protein Data Bank (www.rcsb.org/pdb) under the code 1S5L for PSII structure at 3.5 Å resolution (Ferreira et al., 2004). The overlay cartoon was generated by freeware program Accelrys ViewerLite 4.2.

3. Results

3.1. Biochemical characterization of the PsbH-His PSII complex

Functional integration of the PsbH protein tagged with the His_6 epitope on its N terminus into PSII in PsbH-His strain of *Synechocystis* 6803 has been confirmed by high light treatment. Unlike $PsbH^-$ strain, PsbH-His strain was able to grow at light intensity of 200 μmol (photons) $m^{-2} s^{-1}$ with growth rate comparable to that of wild type (not shown).

His-tagged PSII complex was purified by a single-step Ni^{2+} affinity column chromatography. The PSII fraction was eluted with a concentration of 50 mM imidazole. The polypeptide composition of the purified PsbH-His PSII complex was analyzed by SDS–PAGE (Fig. 1). The PSII complex consisted of at least CP47, CP43, D2, D1, cytochrome b_{559} as confirmed by Western blot (not shown). The presence of PsbH protein in the PSII preparation was probed by immunodetection with anti psbH and anti His antibodies. As shown in Fig. 1, there was a clear shift (about 1 kDa) in the mobility of the PsbH-His protein in comparison to the PsbH caused by the six additional histidines.

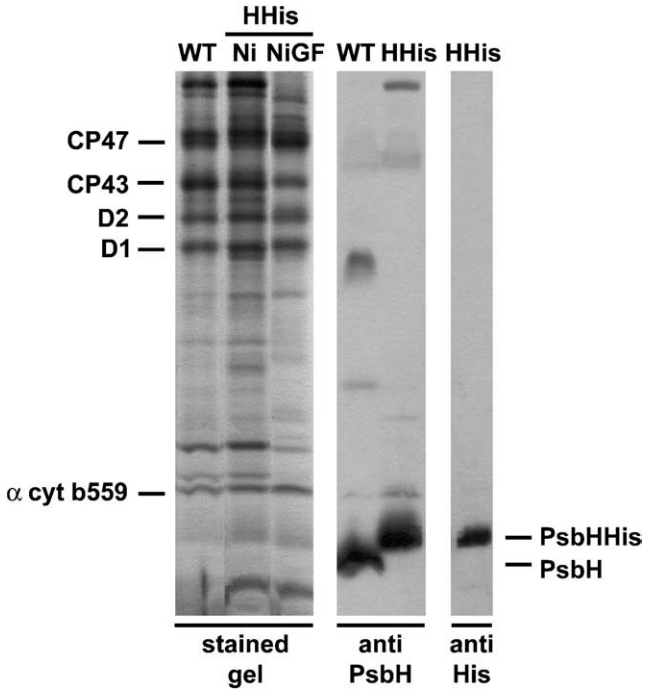

Fig. 1. Protein composition of PSII complex isolated from *Synechocystis* 6803. PSII complex purified from wild type (WT) and the mutant psbH-His strain (HHis) by Ni^{2+} affinity (Ni) followed by gel filtration chromatography (NiGF) was analyzed by SDS–PAGE. Proteins were either stained with Coomassie Blue (stained gel) or blotted onto PVDF membrane and immunodecorated using either antibody against PsbH-GST conjugate (anti-PsbH) or antibody against His_6 epitope (anti-His).

Room temperature absorption spectrum of the PSII fraction is shown in Fig. 2A. The PSII fraction exhibited absorption maxima at 438 nm and 674 nm and lacked the significant absorbance around 550 nm indicating that the sample is free of phycobiliproteins. Seventy-seven Kelvin fluorescence emission spectrum of PSII fraction showed a single emission peak with maximum at 692 nm characteristic for PSII complex (Fig. 2B). The PSII complexes were active in oxygen evolution and yielded $386 \pm 45\ \mu mol(O_2)\ mg(Chl)^{-1}\ h^{-1}$.

The PSII fraction was further purified by gel filtration chromatography (Fig. 2C). Gel filtration analysis of PSII fraction shows a major peak eluting at 18.2 min that corresponds to the dimeric PSII complex with a molecular mass of about 500 kDa. Small peaks eluting at 22 min and 26 min may be interpreted as monomeric PSII complex and free PSII proteins, respectively. For electron microscopy, the dimeric PSII complexes were collected from the maximum of the main peak of the gel filtration.

3.2. Electron microscopy and gold labeling of the PsbH-His PSII complex

To identify the location of the His-tagged PsbH subunit within PSII, the dimeric PSII complexes were immobilized on glow-discharged carbon-coated electron microscopy grid and labeled with Ni–NTA Nanogold (Büchel et al., 2001). The advantage of this labeling lies in a more accurate localization of the targeted site since no additional protein densities are present as compared with conventional immunogold labeling procedures. This approach gave specific labeling of multiple His sites on the protein complexes (Fig. 3). The effectiveness of the procedure was confirmed by carrying out the labeling in a buffer containing 30 mM imidazole which, due to competition with the His-tag for the Ni–NTA sites, abolished any labeling of proteins (Büchel et al., 2001).

Labeled PSII complexes were then negatively stained and visualized in electron microscope. A typical EM images in Fig. 3 clearly show that the preparation contains dispersed particles with uniform size and shape and almost free of contaminants. The image shows that the preparation contained dimeric PSII particles, mostly in their top-view projections (i.e. perpendicular to the original membrane plane). Fig. 3 also shows that only a few PSII dimers exhibited gold label. Although different labeling conditions, such as incubation time, label concentration, pH and temperature were employed to improve gold labeling, no significant changes in the extent of labeling were observed (not shown).

3.3. Image analysis

To reveal the exact location of the gold label within PSII dimers, both labeled and unlabeled particles were extracted from the micrographs, and separately aligned, treated with multivariate statistical analysis and classified. The most representative class averages of both labeled and unlabeled particles are depicted in Fig. 4. Although no symmetry has been imposed during the image analysis clearly two-fold rotational symmetry around the center of the complex is visible. The class averages were similar in size and shape, and they closely resembled PSII core complexes without the His-tagged PsbH protein (Boekema et al., 1995; Bumba et al., 2004; Kuhl et al., 1999; Nield et al., 2000). All the projections had the same type of handedness and no mirror images were detected, thus indicating preferred orientation of the PSII dimers with their stromal side to the carbon support film. Therefore, the relatively low number of labeled particles probably reflects the preferential binding of the PSII particles. Since a His-tag of the PsbH protein is located on the stromal side of the complex, the labeling site is inaccessible when the particles are orientated with their stromal sides to the carbon support film. A final sum of labeled PSII core complexes is presented in Fig. 4E. The averaged top-view projection indicates a particle with single label located at the periphery of the complex. The resolution of the final projections was calculated by means of the Fourier ring correlation method (van Heel, 1987) and found to be 26 Å for class average

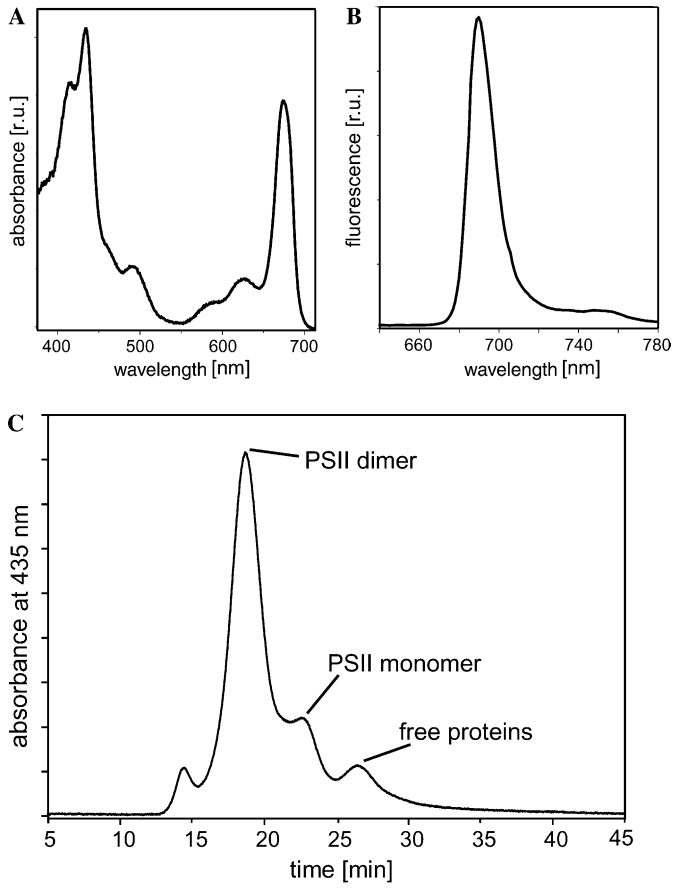

Fig. 2. Absorbance and fluorescence properties of PSII complex with His-tagged PsbH protein isolated from *Synechocystis* 6803: (A) room temperature absorbance spectrum; (B) fluorescence emission spectrum at 77 K excited at 430 nm; (C) gel-filtration chromatography elution profile of PSII fraction obtained from Ni^{2+} affinity column chromatography. The chromatogram was detected at 435 nm for chlorophyll containing proteins.

of gold labeled PSII dimers and 21 Å for unlabeled class averages.

4. Discussion

Here we present the study to identify the location of the PsbH protein within the PSII core complex. The combination of Ni–NTA Nanogold labeling of His-tagged protein and single particle analysis provides an excellent tool to localize protein subunits within a multi-subunit protein complex (Büchel et al., 2001). The advantage of this labeling lies in a more accurate localization of the targeted site since no additional protein densities are present as compared with conventional immunogold labeling procedures. Although low number of labeled particles was collected from the micrographs this approach gave specific labeling of His-tag sites, enabling us to locate the PsbH in the PSII core complex (Fig. 3).

Biochemical and spectroscopic characterization of isolated PSII complex with His-tagged protein revealed that incorporation of recombinant PsbH protein into PSII has no evident effect on its structure and function. The PSII dimers were active in oxygen evolution indicating the integrity of the extrinsic polypeptides located at the lumenal side of the complex. In addition, a comparison of the top-view projection map of the dimeric PSII complex isolated from the wild type with that of the PsbH-His PSII complex suggested identical size and shape of the complex (not shown).

His-tag of the PsbH protein is linked to the N-terminal end of the polypeptide and faces the stromal side of the PSII complex. In our experiments, electron microscopy and image analysis revealed that both labeled and unlabeled PSII dimers attach preferentially with their stromal sides to the carbon support film (Fig. 5). This is in contrast with the results obtained using PSII core complexes isolated from *C. reinhardtii*, where the gold labeled complexes bind to the electron microscopy grid by the lumenal surface. This is probably one of the reasons why we were able to observe only one label per whole PSII complex compared to the results of Büchel et al. (2001) who had labeled both sides of the PSII complex.

We suppose that in our case only those particles which were tilted in respect to the carbon support film were labeled, allowing the gold particles to reach the

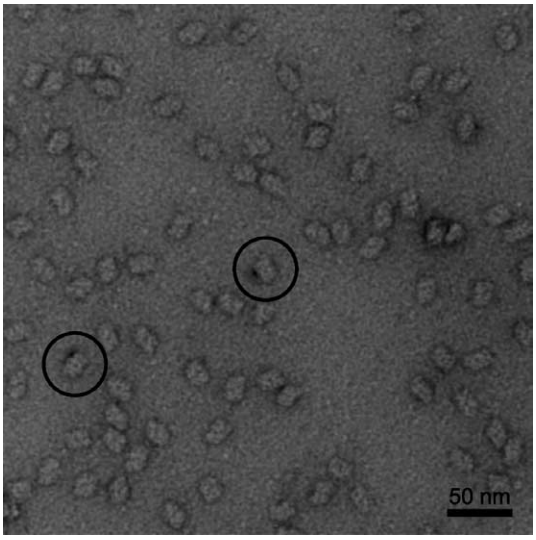

Fig. 3. Electron micrographs of dimeric PSII complexes labeled with Ni–NTA Nanogold and negatively stained with 0.75% uranyl acetate. The labeled particles are in circles.

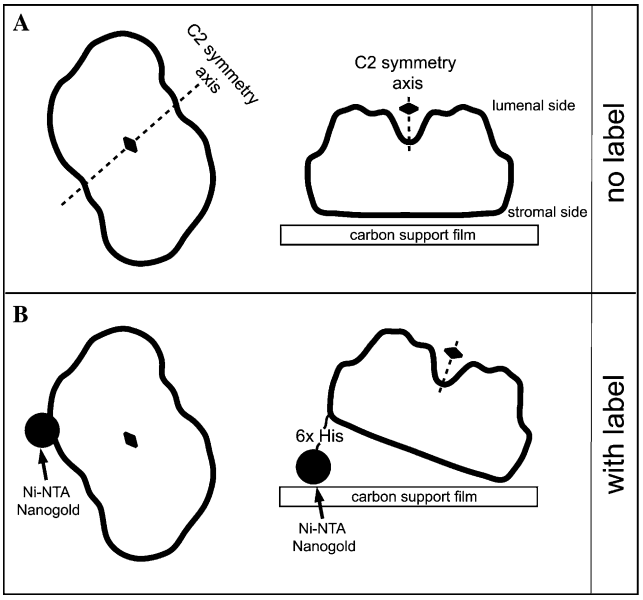

Fig. 5. Schematic representation of the preferred orientations of unlabeled (A) and labeled (B) PSII core complexes with respect to the carbon support film. The gold labels are shown as black circles. The C2 symmetry axis of PSII dimer are shown as twofold symbols and broken lines. The labeled particle is tilted in respect to the support carbon film to expose His-tag labeling site.

binding His-tag site as it is demonstrated in Fig. 5B. Another reason for the lower gold-label affinity may be the fact that in cyanobacteria the N terminus of the PsbH protein is 19 amino acids shorter compared to the *C. reinhardtii*, and thus, the potential labeling site is located more inside the complex. Such location might be partially covered by neighboring amino acid side chains making the His-tag labeling site less accessible to the gold label. On the other hand, the shorter N terminus of the *Synechocystis* PsbH protein enabled us to identify the location of the His site more precisely within the PSII complex. A careful comparison of the location of the gold clusters in *C. reinhardtii* and *Synechocystis* PSII

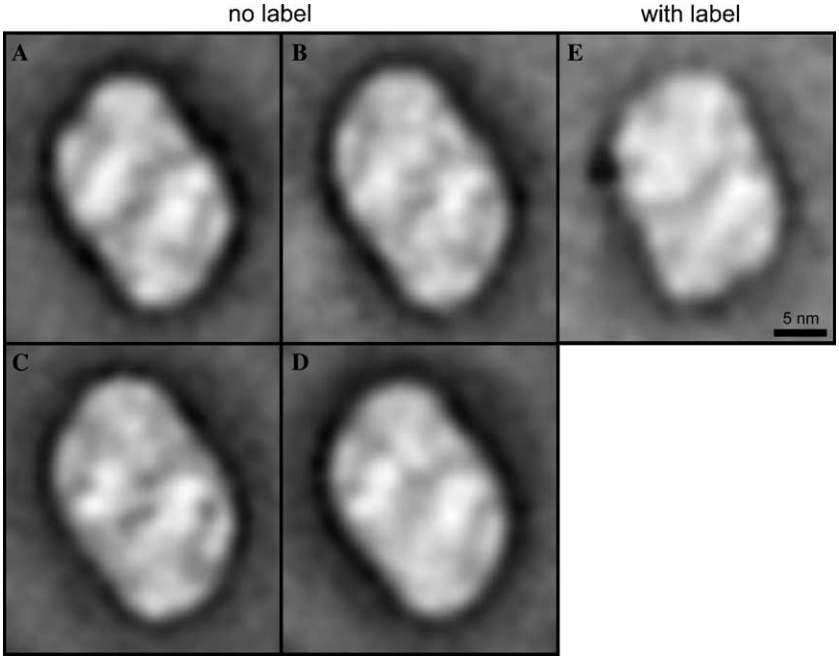

Fig. 4. Single particle analysis of top-view projections of unlabeled (A–D) and PsbH-His PSII core complex labeled with Ni–NTA Nanogold (E). The projections are presented as facing from the lumenal side of the thylakoid membrane and the number of summed images is: 530 (A), 483 (B), 385 (C), 542 (D), and 185 (E). The overall dimensions of the class average of the unlabeled PSII dimers are 23 × 16 nm, whereas the dimension of labeled PSII dimer is 23 × 17 nm.

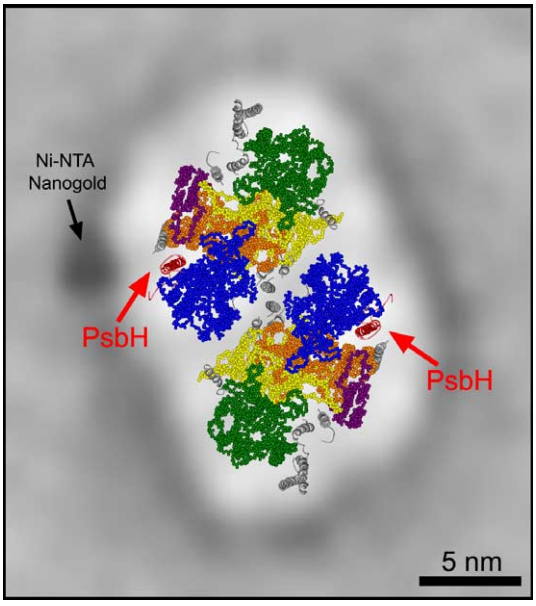

Fig. 6. Top-view projection map of the PsbH-His PSII core complex labeled with Ni–NTA Nanogold overlaid with the cyanobacterial X-ray model of the dimeric PSII core complex resolved at 3.5 Å resolution (Ferreira et al., 2004), Protein Data Bank accession number 1S5L. Carbon atoms and amino acid side chains of the major PSII subunits are in color spacefill representation; i.e. CP47 (blue), CP43 (green), D1 (yellow), D2 (orange) and cytochrome b_{559} (violet). Single transmembrane helices assigned to low molecular weight PSII subunits are represented as solid ribbons in gray color except for subunits PsbH (in red). Heteroatoms and extrinsic proteins are not shown. The Ni–NTA Nanogold label is observed only at the one side of the complex (black arrow). Since PSII particle is dimeric two PsbH subunits are present within two fold rotational symmetry around the center of the complex (red arrows).

complexes revealed that gold label in *Synechocystis* preparation is slightly shifted with respect to the longer edge of the complex.

At the present time, there are three published X-ray crystal structures of cyanobacterial PSII at, respectively, 3.8 Å (Zouni et al., 2001), 3.7 Å (Kamiya and Shen, 2003) and 3.5 Å resolution (Ferreira et al., 2004). All the three models are almost identical with respect to the location of the major PSII subunits and the arrangement of cofactors. Significant differences exist in the assignment of the single transmembrane helices representing the low molecular mass PSII subunits (Fig. 6, grey helices). In case of PsbH subunit, Zouni et al. (2001) tentatively assigned the PsbH protein to one of the three helices clustered at the contact of two monomers, while Kamiya and Shen (2003) placed the PsbH protein on the outside of the monomer close to the D2 protein. In the latest model, Ferreira et al. (2004) assigned the PsbH protein as a single transmembrane helix next to the CP47 subunit.

To locate the PsbH protein within the PSII complex we have overlaid a model of transmembrane helix organization of PSII into top-view projection map of the gold labeled PSII particle. Fig. 6 shows that Ni–NTA gold label is found to be close to the transmembrane helices of the CP47 protein. This would suggest that the PsbH protein corresponds to a single transmembrane helix in the vicinity of the CP47 protein. Although we have detected only one label attached to the PSII core complex, the observed particle is a PSII dimer and, therefore, two PsbH subunits are present within a two-fold rotational symmetry around the center of the complex (Fig. 6, red helices). The location of the PsbH subunit is in good agreement with the assignment of the PsbH subunit in the model of Ferreira et al. (2004) and it seems highly likely that single transmembrane helix close to the CP47 subunit corresponds to the PsbH protein.

Our results are also supported by the fact that the PsbH protein plays important role in the biogenesis and structure of PSII complex (Komenda et al., 2004; Suorsa et al., 2004). Deletion of the PsbH subunit in *C. reinhardtii* leads to the complete disappearance of PSII complex from the thylakoid membrane documenting its role in the stable assembly of PSII complex (O'Connor et al., 1998; Summer et al., 1997). A role of the PsbH protein in the stabilization of the PSII complex has been recently supported by recent data in which the isolated PSII complex from the *psbH* deletion mutant of *Synechocystis* 6803 was subjected to non-denaturing electrophoresis (Komenda et al., 2002). In contrast to the isolated PSII complex from the wild type, a large amount of the reaction center complex D1–D2-cyt b_{559} appeared on the gel indicating that the PsbH protein stabilizes the binding of the CP47 subunit to the D1–D2 heterodimer. Such a role could also explain the instability of the PSII core complex in *C. reinhardtii*, since weak binding of CP47 to the heterodimer could allow a fast proteolysis of PSII subunits before the complex becomes fully assembled (Komenda et al., 2003).

5. Conclusions

Ni–NTA Nanogold label consists of a gold cluster coupled to Ni^{2+}–NTA (nitrilotriacetic acid) (Hainfeld et al., 1999). The high binding affinity of Ni^{2+} to multiple histidine (His) sites was employed to label His-tagged PsbH protein. Using a mutant of *Synechocystis* 6803 with a His-tag on the N terminus of the PsbH subunit, we were able to identify the location of the PsbH subunit within the PSII complex in electron microscope. Our analysis suggests that labeling of His sites using Ni–NTA gold cluster is a powerful approach to locate specific proteins within multisubunit protein complex.

Acknowledgments

The work was supported by the project MSM6007665808 of the Ministry of Education, Youth

and Sports of the Czech Republic. Supports from Institutional Research Concept of the Academy of Sciences of the Czech Republic AV0Z50510513 and AV0Z50200510 are also acknowledged.

References

Bennet, J., 1977. Phosphorylation of chloroplast membrane polypeptides. Nature 269, 344–346.

Boekema, E.J., Hankamer, B., Bald, D., Kruip, J., Nield, J., Boonstra, A.F., Barber, J., Rögner, M., 1995. Supramolecular structure of the photosystem II complex from green plants and cyanobacteria. Proc. Natl. Acad. Sci. USA 92, 175–179.

Büchel, C., Morris, E., Orlova, E., Barber, J., 2001. Localization of the PsbH subunit in photosystem II: A new approach using labeling of His-tags with a Ni^{2+}-NTA gold cluster and single particle analysis. J. Mol. Biol. 312, 371–379.

Bumba, L., Havelková-Doušová, H., Hušák, M., Vácha, F., 2004. Structural characterization of photosystem II complex from red alga *Porphyridium cruentum* retaining extrinsic subunits of the oxygen-evolving complex. Eur. J. Biochem. 271, 2967–2975.

Bumba, L., Vácha, F., 2003. Electron microscopy in structural studies of photosystem II. Photosynth. Res. 77, 1–19.

Dedner, N., Meyer, H.E., Ashton, C., Wildner, G.F., 1988. N-terminal sequence analysis of the 8-kDa protein in *Chlamydomonas reinhardtii*—localization of the phosphothreonine. FEBS Lett. 236, 77–82.

Ferreira, K.N., Iverson, T.M., Maghlaoui, K., Barber, J., Iwata, S., 2004. Architecture of the photosynthetic oxygen-evolving center. Science 303, 1831–1838.

Frank, J., Radermacher, M., Penczek, P., Zhu, J., Li, Y.H., Ladjadj, M., Leith, A., 1996. SPIDER and WEB: processing and visualization of images in 3D electron microscopy and related fields. J. Struct. Biol. 116, 190–199.

Hainfeld, J.F., Liu, W., Halsey, C.M.R., Freimuth, P., Powell, R.D., 1999. Ni–NTA gold clusters target His-tagged proteins. J. Struct. Biol. 127, 185–198.

Halbhuber, Z., Petrmichlová, Z., Alexciev, K., Thulin, E., Štys, D., 2003. Overexpression and purification of recombinant membrane PsbH protein in *Escherichia coli*. Protein Expr. Purif. 32, 18–27.

Hankamer, B., Morris, E.P., Nield, J., Carne, A., Barber, J., 2001a. Subunit positioning and transmembrane helix organisation in the core dimer of photosystem II. FEBS Lett. 504, 142–151.

Hankamer, B., Morris, E.P., Nield, J., Gerle, C., Barber, J., 2001b. Three-dimensional structure of the photosystem II core dimer of higher plants determined by electron microscopy. J. Struct. Biol. 135, 262–269.

Harauz, G., Boekema, E., van Heel, M., 1988. Statistical image analysis of electron micrographs of ribosomal subunits. Methods Enzymol. 164, 35–49.

Kamiya, N., Shen, J.R., 2003. Crystal structure of oxygen-evolving photosystem II from *Thermosynechococcus vulcanus* at 3.7 Å resolution. Proc. Natl. Acad. Sci. USA 100, 98–103.

Komenda, J., Barber, J., 1995. Comparison of psbO and psbH deletion mutants of Synechocystis PCC6803 indicates that degradation of D1 protein is regulated by the Q_B site and dependent on protein-synthesis. Biochemistry 34, 9625–9631.

Komenda, J., Lupinkova, L., Kopecky, J., 2002. Absence of the psbH gene product destabilizes photosystem II complex and bicarbonate binding on its acceptor side in Synechocystis PCC6803. Eur. J. Biochem. 269, 610–619.

Komenda, J., Reisinger, V., Muller, B.C., Dobakova, M., Granvogl, B., Eichacker, L.A., 2004. Accumulation of the D2 protein is a key regulatory step for assembly of the photosystem II reaction center complex in *Synechocystis* PCC6803. J. Biol. Chem. 279, 48620–48629.

Komenda, J., Stys, D., Lupinkova, L., 2003. The PsbH protein of photosystem 2. Photosynthetica 41, 1–7.

Kuhl, H., Rogner, M., van Breemen, J.F.L., Boekema, E.J., 1999. Localization of cyanobacterial photosystem II donor-side subunits by electron microscopy and the supramolecular organization of photosystem II in the thylakoid membrane. Eur. J. Biochem. 266, 453–459.

Lagarde, D., Beuf, L., Vermaas, W., 2000. Increased production of zeaxanthin and other pigments by application of genetic engineering techniques to *Synechocystis* sp. strain PCC6803. Appl. Environ. Microbiol. 66, 64–72.

Mayes, S.R., Barber, J., 1991. Primary structure of the *psbN–psbH–petC–petA* gene cluster of the cyanobacterium *Synechocystis* PCC6803. Plant Mol. Biol. 17, 289–293.

Mayes, S.R., Dubbs, J.M., Vass, I., Hideg, E., Nagy, L., Barber, J., 1993. Further characterization of the psbH locus of *Synechocystis* sp. PCC 6803—inactivation of psbH impairs Q(A) to Q(B) electron-transport in photosystem 2. Biochemistry 32, 1454–1465.

Michel, H.P., Bennett, J., 1987. Identification of the phosphorylation site of an 8.3 kDa protein from photosystem II of spinach. FEBS Lett. 212, 1123–1130.

Nield, J., Kruse, O., Ruprecht, J., da Fonseca, P., Buchel, C., Barber, J., 2000. 3D maps of *Chlamydomonas reinhardtii* and *Synechococcus elongatus* photosystem II complexes allow for comparison of their OEC organisation. J. Biol. Chem. 275, 27940–27946.

O'Connor, H.E., Ruffle, S.V., Cain, A.J., Deak, Z., Vass, I., Nugent, J.H.A., Purton, S., 1998. The 9-kDa phosphoprotein of photosystem II. Generation and characterisation of *Chlamydomonas* mutants lacking PSII-H and a site-directed mutant lacking the phosphorylation site. Biochim. Biophys. Acta 1364, 63–72.

Shi, L.X., Lorkovic, Z.J., Oelmuller, R., Schröder, W.P., 2000. The low molecular mass PsbW protein is involved in the stabilization of the dimeric photosystem II complex in *Arabidopsis thaliana*. J. Biol. Chem. 275, 37945–37950.

Shi, L.X., Schröder, W.P., 2004. The low molecular mass subunits of the photosynthetic supracomplex, photosystem II. Biochim. Biophys. Acta 1608, 75–96.

Shinozaki, K., Ohme, M., Tanaka, M., Wakasugi, T., Hayashida, N., Matsubayashi, T., Zaita, N., Chungwongse, J., Obokata, J., Yamagushishinozaki, K., Ohto, C., Torazawa, K., Meng, B.Y., Sugita, M., Deno, H., Kamogashira, T., Yamada, K., Kusuda, J., Takaiwa, F., Kato, A., Tohdon, N., Shimada, H., Sugiura, M., 1986. The complete nucleotide sequence of tobacco chloroplast genome—its gene organization and expression. EMBO J. 5, 2043–2049.

Summer, E.J., Schmid, V.H.R., Bruns, B.U., Schmidt, G.W., 1997. Requirement for the H phosphoprotein in photosystem II of *Chlamydomonas reinhardtii*. Plant Physiol. 113, 1359–1368.

Suorsa, M., Regel, R., Paakkarinen, V., Battchikova, N., Herrmann, R.G., Aro, E.-M., 2004. Protein assembly of photosystem II and accumulation of subcomplexes in the absence of low molecular mass subunits PsbL and PsbJ. Eur. J. Biochem. 271, 96–107.

Swiatek, M., Kuras, R., Sokolenko, A., Higgs, D., Olive, J., Cinque, G., Muller, B., Eichacker, L.A., Stern, D.B., Bassi, R., Herrmann, R.G., Wollman, F.A., 2001. The chloroplast gene *ycf9* encodes a photosystem II (PSII) core subunit, PsbZ, that participates in PSII supramolecular architecture. Plant Cell 13, 1347–1367.

van Heel, M., 1987. Similarity between images. Ultramicroscopy 21, 95–100.

van Heel, M., Frank, J., 1981. Use of multivariate statistics in analyzing the images of biological macromolecules. Ultramicroscopy 6, 187–194.

Vener, A.V., Harms, A., Sussman, M.R., Vierstra, R.D., 2001. Mass spectrometric resolution of reversible protein phosphorylation in photosynthetic membranes of *Arabidopsis thaliana*. J. Biol. Chem. 276, 6959–6966.

Zouni, A., Witt, H.T., Kern, J., Fromme, P., Krauss, N., Saenger, W., Orth, P., 2001. Crystal structure of photosystem II from *Synechococcus elongatus* at 3.8 Å resolution. Nature 409, 739–743.